

## Article

# Hg/Se/PbSO<sub>4</sub> Recovery by Microwave-Intensified HgSe Pyrolysis from Toxic Acid Mud

Hanlin Zeng<sup>1,2,3</sup>, Peng Liu<sup>1,2,3</sup>, Yan Hong<sup>1,2,3</sup>, Kun Yang<sup>1,2,3,\*</sup> and Libo Zhang<sup>1,2,3,\*</sup> 

- <sup>1</sup> Faculty of Metallurgical and Energy Engineering, Kunming University of Science and Technology, Kunming 650093, China; hanlinzeng94@126.com (H.Z.); tbagmo@126.com (P.L.); 17704702287@sina.cn (Y.H.)
- <sup>2</sup> State Key Laboratory of Complex Nonferrous Metal Resources Clean Utilization, Kunming University of Science and Technology, Kunming 650093, China
- <sup>3</sup> Key Laboratory of Unconventional Metallurgy, Ministry of Education, Kunming 650093, China
- \* Correspondence: truepsyche@sina.com (K.Y.); zhanglibopaper@126.com (L.Z.)

**Abstract:** The acid mud produced in the nonferrous smelting process is a hazardous waste, which mainly consists of elements Hg, Se, and Pb. Valuable metal (Hg/Se/Pb) can be recovered from acid mud by heat treatment. For safe disposal of the toxic acid mud, a new resource utilization technology by microwave roasting is proposed in this paper. The reaction mechanisms were revealed through thermodynamics and thermogravimetric analysis, which showed that the main reaction was the oxidative pyrolysis of HgSe in the process of roasting. Moreover, the mercury removal effects of acid mud by microwave heating and conventional heating were studied, the recovery rate of mercury by microwave heating for 30 min at 400 °C was 99.5%: far higher than that of conventional heating for 30 min at 500 °C (44.3%). This was due to the high dielectric constant of HgSe, as microwaves can preferentially heat HgSe and reduce the adsorption energy of HgSe on the surface of PbSO<sub>4</sub> blocks, thus strengthening the pyrolysis process of HgSe and reducing energy consumption. The preferable prototyping technology for resource utilization of toxic acid mud should be microwave roasting. This study is of great significance for the realization of mercury pollution reduction and for green production of lead-zinc smelting.



**Citation:** Zeng, H.; Liu, P.; Hong, Y.; Yang, K.; Zhang, L. Hg/Se/PbSO<sub>4</sub> Recovery by Microwave-Intensified HgSe Pyrolysis from Toxic Acid Mud. *Metals* **2022**, *12*, 1038. <https://doi.org/10.3390/met12061038>

Academic Editor: Antonije Onjia

Received: 9 May 2022

Accepted: 15 June 2022

Published: 17 June 2022

**Publisher's Note:** MDPI stays neutral with regard to jurisdictional claims in published maps and institutional affiliations.



**Copyright:** © 2022 by the authors. Licensee MDPI, Basel, Switzerland. This article is an open access article distributed under the terms and conditions of the Creative Commons Attribution (CC BY) license (<https://creativecommons.org/licenses/by/4.0/>).

**Keywords:** acid mud; resource recovery; microwave heating; conventional heating; mercury pollution reduction

## 1. Introduction

Mercury's polluting features are its persistence, mobility, high toxicity, and biological accumulation [1–3], and it is a pollutant that has attracted worldwide attention. Mercury-containing wastes are considered hazardous in waste management [4]. Mercury is associated with sphalerite, although the content is low, but with the increase in zinc smelting scale, mercury gradually accumulates in the roasting dust [5,6]. In the roasting process of sphalerite, due to the boiling point of mercury, selenium and lead levels are lower than other metals: when the roasting temperature reaches above 800 °C, most of the mercury, selenium, and lead in sphalerite volatilize into the flue dust, then mercury-containing dust is collected into the dust-collecting system. Finally, mercury-containing dust is washed to form mercury-containing acid mud (MAM) [7–9] (Figure 1). The mercury content of MAM is about 35%, and according to the US Land Disposal Restrictions, MAM is a type of “high mercury waste” (total Hg content > 260 mg/kg) [10]. A zinc smelter in Yunnan produces 200 tons of MAM every year. The amount of MAM is increasing every year, and the mercury content of MAM is also gradually increasing. The storage of MAM constitutes waste of resources and potential threat to the survival environment and human. Therefore, how to treat MAM in a harmless way and realize the recycling of metals in MAM is of great significance to the green production of the lead-zinc smelting process.



**Figure 1.** Background process of the production of MAM.

At present, two commonly used conventional methods are mainly thermal treatment and acid leaching. Thermal treatment method was investigated by Lei [11], who heated the mixture of MAM and CaO at temperature 650 °C for 90 min, so mercury evaporated and collected in the condenser. Though the mercury recovery rate reached 99.4%, this method consumed large amounts of energy for its low heating efficient and produced a large amount of slag. Zhou [12] used  $\text{KClO}_3/\text{HCl}$  to leach MAM and precipitate the mercury with NaOH to obtain  $\text{HgO}$  which can be turned into  $\text{Hg}^0$  by roasting; however, only 72.73% mercury was recovered. Zhang [13] leached MAM with  $\text{Na}_2\text{S}$  solution for the first stage, and then leached MAM with NaOH solution for the second stage. The  $\text{HgS}_2^{2-}$  formed during leaching was finally reduced by aluminum powder to obtain  $\text{Hg}^0$ . The mercury recovery rate by this method was 91.87%. However, it takes 4 h and the steps are complicated. It can be seen that the acid leaching method is cumbersome and time-consuming. Currently, the U.S. Environmental Protection Agency recommends heat treatment to remove mercury from these “high mercury wastes” [14–16]. Due to the good microwave absorption ability of mercury compounds [17], microwaves could heat mercury compounds selectively, and remove mercury efficiently.

A microwave is a kind of the electromagnetic wave with a frequency from 300 MHz–300 GHz and wavelength 1 mm–10 m [18]. Microwave heating could heat the materials (microwave absorbing materials) selectively and intensified the related reactions [19–21], this heating method has been widely used in green chemistry [22]. Specifically speaking, the advantages of microwave heating are that it is rapid, volumetric, and selective [23–25]. Compared with conventional heating systems, microwave heating could heat directly within the material [26] and require less heating time [27,28], and therefore be more efficient. Due to the large amount of MAM, it is necessary to find a proper heating method to recovery the valuable metals and release the environmental pressure. Considering the good microwave heating behavior of MAM, microwave heating is suitable to treat MAM.

In view of the high energy consumption in the recent MAM treatment, a new resource utilization technology was proposed for MAM by microwave heating in this paper. Busto et al. [29] and Liu [15] researched that the effect of treatment temperature (300–800 °C) on mercury removal was greater than that of treatment time (10–120 min). So, the reaction mechanism in the microwave heating process of MAM at different temperatures in details was studied in this work. By comparing the mercury recovery rate and remaining roasted phases, the advantage of microwave treatment is analyzed. The microwave treatment with MAM is a key factor for the realization of green production in the lead-zinc smelting process which has great research value.

## 2. Experimental

### 2.1. Materials

The MAM was obtained from a lead-zinc smelter (Chihong Company, Yunnan, China) of the Yunnan province in China, MAM was pre-processed and ground to a powder size under  $8.47 \mu\text{m}$  in kibbler. The composition of the dried MAM was determined by X-Ray Fluorescence Spectrometer (Tianrui Instrument Co., Ltd, Taizhou, China). The main chemical compositions of MAM are shown in Table 1. MAM has a high grade of Hg, Pb, and Se, with total amount exceeding 80%, which can be classified into high toxic acid mud. According to the X-ray Diffraction (XRD) patterns of MAM (Figure 2a) analysis, the main phases of MAM are HgSe and PbSO<sub>4</sub>. Hg4f X-ray Photoelectron Spectroscopy (XPS) detailed spectrum of MAM is shown in Figure 2b, the binding energy of Hg4f can be divided into two peaks, 100.6 eV (Hg4f5/2) and 104.6 eV (Hg4f7/2), which demonstrated the HgSe phase [30,31]. According to the results of the field emission scanning electron microscope (Figure 2c), the positions of the two elements of mercury and selenium are well matched, which is consistent with the XRD patterns phases and Hg4f XPS detailed spectrum results. HgSe powder is dispersedly attached to the surface of PbSO<sub>4</sub> blocks with flocculent structure.

**Table 1.** Chemical compositions of MAM.

Compositions	Hg	Se	Pb	S	Ca	Fe	Zn
Content/wt%	34.82	13.15	33.07	5.42	0.15	0.15	0.11

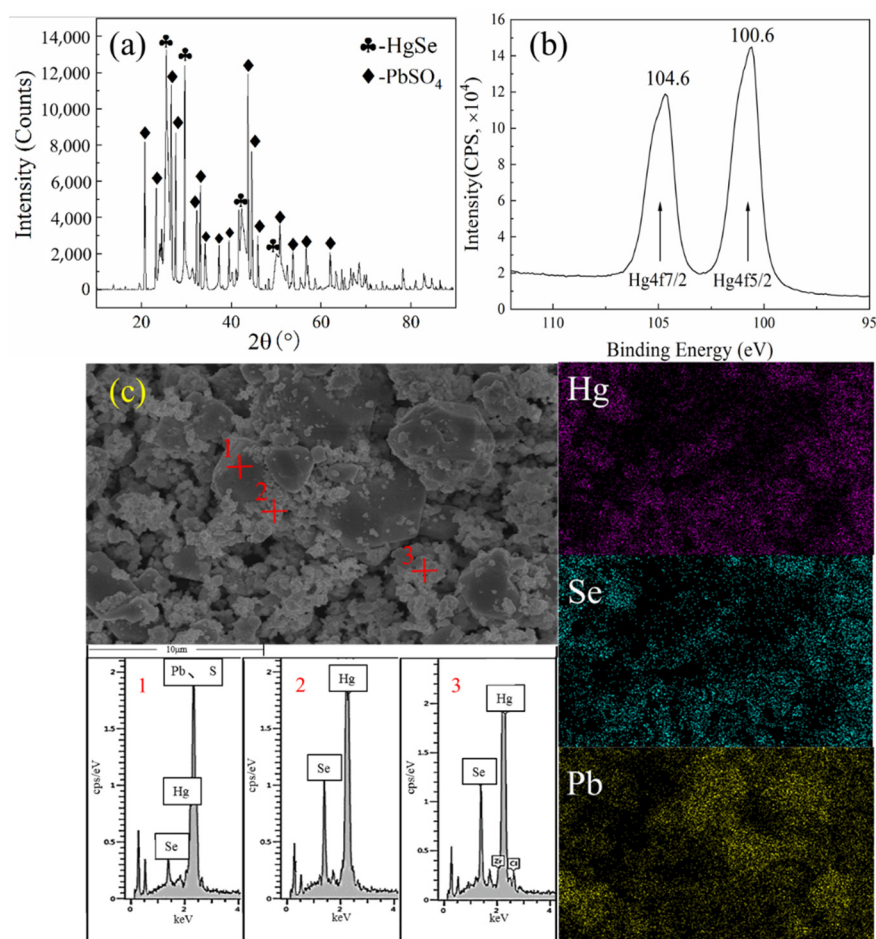


**Figure 2.** MAM characterization results: (a) XRD patterns of MAM; (b) Hg 4f XPS detailed spectrum of MAM; (c) FESEM-EDS images of MAM.

## 2.2. Experiments of Microwave and Conventional Heating

Two heating methods were used to process MAM. The power of microwave heating is 800 W, and conventional heating 2700 W. Except for the different heating methods, the other experimental conditions were the same. Details are as follows: the atmosphere of the reaction process was air, and the flow rate was 0.5 L/min, the amount of MAM used in each experiment is 20 g, and a ceramic crucible was used for loading. A sheltered type-K thermocouple was plugged into the center of the sample to measure the temperature, and the reaction temperatures were 300, 350, 400, 450, and 500 °C. The reaction time of each experiment was fixed at 30 min. The equipment flow chart is shown in Figure 3. Equipment 1,2 are an air intake system, equipment 3,4 are a heating temperature measurement system, 5 is MAM, equipment 6 is a mercury recovery device, equipment 7–10 are a tail gas treatment system. Mercury recovery experiments were performed in a tube microwave furnace at 2.45 GHz and a tube muffle furnace, respectively. The generated  $\text{Hg}^0$  (g) was condensed by the water condenser to form mercury beads for recovery.  $\text{SeO}_2$  (g) was dissolved in the water condenser and  $\text{H}_2\text{SeO}_3$  was generated, which realized the separation and recovery of mercury and selenium. For safety, some gas-washing bottles containing 4%  $\text{KMnO}_4$ /10%  $\text{H}_2\text{SO}_4$  solution,  $\text{Na}_2\text{S}$  solution,  $\text{NaOH}$  solution, and activated carbon mixed with sulfur powder were attached to the rear of the condenser to absorb exhaust gas.

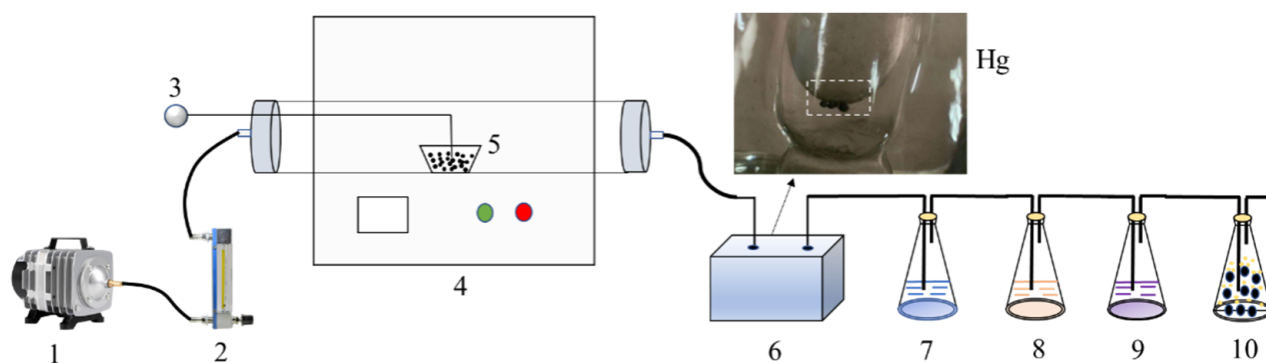


**Figure 3.** Schematic diagram of microwave/conventional heating equipment. (1) Air pump; (2) Flowmeter; (3) Type-K thermocouple; (4) Furnace (microwave furnace or muffle furnace); (5) Ceramic crucible; (6) Water condenser; (7) 4%  $\text{KMnO}_4$ /10%  $\text{H}_2\text{SO}_4$ ; (8)  $\text{Na}_2\text{S}$  solution; (9)  $\text{NaOH}$  solution; (10) Activated carbon with sulfur powder.

After the experiment, the samples were cooled to room temperature, and then tested and characterized. Due to the collected mercury being hard to accurately weigh, mass conservation was used to calculate the recovery rate of mercury. The recovery rate of mercury was calculated using the below Equation (1):

$$x = \frac{m_1 \cdot \omega_1 - m_2 \cdot \omega_2}{m_1 \cdot \omega_1} \quad (1)$$

where  $m_1$  is the weight of before roasting MAM (g);  $m_2$  is the weight of after roasting MAM (g);  $\omega_1$  is the content of mercury before roasting MAM (%);  $\omega_2$  is the content of Hg after roasting MAM (%); and  $x$  is the recovery rate of mercury (%).

## 2.3. Material Characterization

The FESEM images were taken by field emission filament scanning electron microscope (Nova-Nano SEM450, FEI Company, Hillsboro, OR, USA). The acceleration voltage was set at 30 KV, and the working distance was kept between 2.8 and 3.5 mm. XRD patterns of MAM detected by Rigaku D/MXA-3B (Malvern Panalytical, Shanghai, China) with  $\text{Cu K}\alpha$  radiation at 40 kV and 40 mA, a scan rate of  $4^\circ \text{min}^{-1}$  was applied to record a pattern in the  $2\theta$  range of  $10\text{--}90^\circ$ . In addition, the thermochemical characteristics of MAM were examined by a high-temperature TGA thermogravimetric analyzer (TGA/DSC 1/1600,

METTLER TOLEDO, Switzerland), at a heating rate of 10 °C/min from 30–800 °C, with air flow (60 mL/min). X-ray Photoelectron Spectroscopy was detected by *K-Alpha*<sup>+</sup> electron spectrometer (Thermo Fisher Scientific, Waltham, MA, USA) to determine the surface chemical composition of materials. The dielectric properties of MAM were measured by a dielectric device (Agilent-E5071C, Innovation of Zhide, Beijing, China) [32,33].

### 3. Results and Discussion

#### 3.1. Thermodynamics Analysis

Thermodynamic data of related reactions (2)–(5) were calculated by Factsage software 7.2 (GTT, Herzogenrath, Germany) [34]. In Figure 4, The Gibbs free energy values  $\Delta G^\theta$  of reaction (2) is negative in the temperature range from 0–600 °C, indicating reaction (2) might occur in the temperature range from 0–600 °C. When the temperature was high enough, reaction (3) ( $T > 338.7$  °C,  $\Delta G^\theta < 0$ ) and reaction (4) ( $T > 357.3$  °C,  $\Delta G^\theta < 0$ ) started.

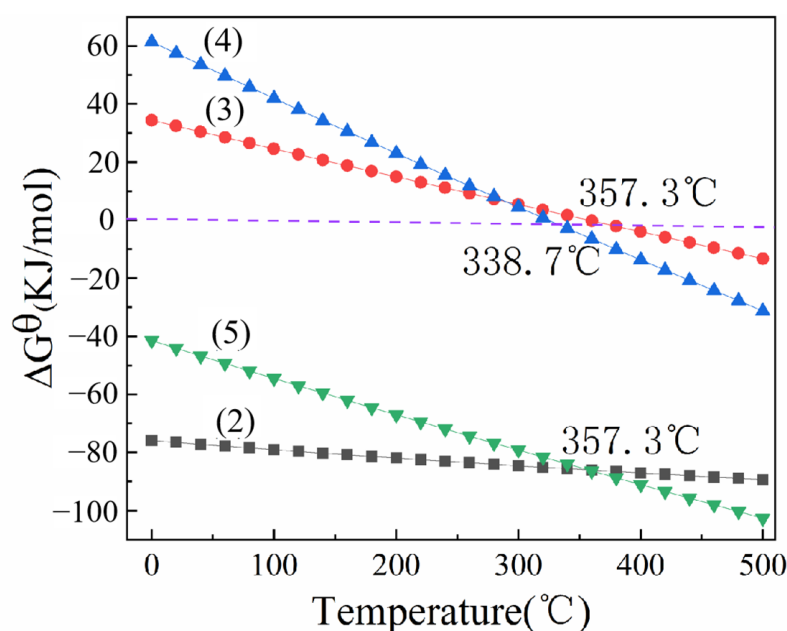
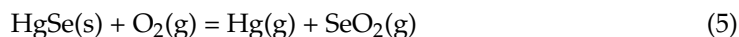
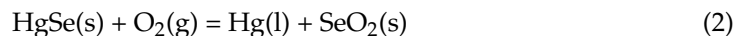


**Figure 4.** Relationships between Gibbs free energy of the reaction and temperature.

The temperature of the intersection point of the  $\Delta G^\theta$  curve of reaction (2) and the  $\Delta G^\theta$  curve of reaction (5) is 357.3 °C. When the temperature is higher than 357.3 °C, both phases of  $\text{Hg}^0$  and  $\text{SeO}_2$  are transformed into gas phase, the free energy values  $\Delta G^\theta$  of reaction (5) is lower than that of reaction (2), indicating that reaction (5) is more likely to occur than reaction (2). The chemical reaction equations are as follows.



#### 3.2. Thermogravimetric Analysis

The decomposition and volatilization of mercury compounds in MAM corresponded the temperature from 300 to 500 °C in the TG curve (Figure 5a). Based on thermodynamic calculation results (Figure 4), reaction (2) and (5) may occur at room temperature; however, for the adsorption of HgSe on the surface of  $\text{PbSO}_4$  blocks, the pyrolysis of HgSe started at 300 °C. As the temperature increases, (1) the equilibrium constant of the Arrhenius equation increases; (2) the adsorption ability of the surface of  $\text{PbSO}_4$  blocks to HgSe

gradually decreases, and the adsorption energy decreases. The two phenomena led to HgSe removal from the surface of PbSO<sub>4</sub> blocks and the beginning of pyrolysis at 300 °C.

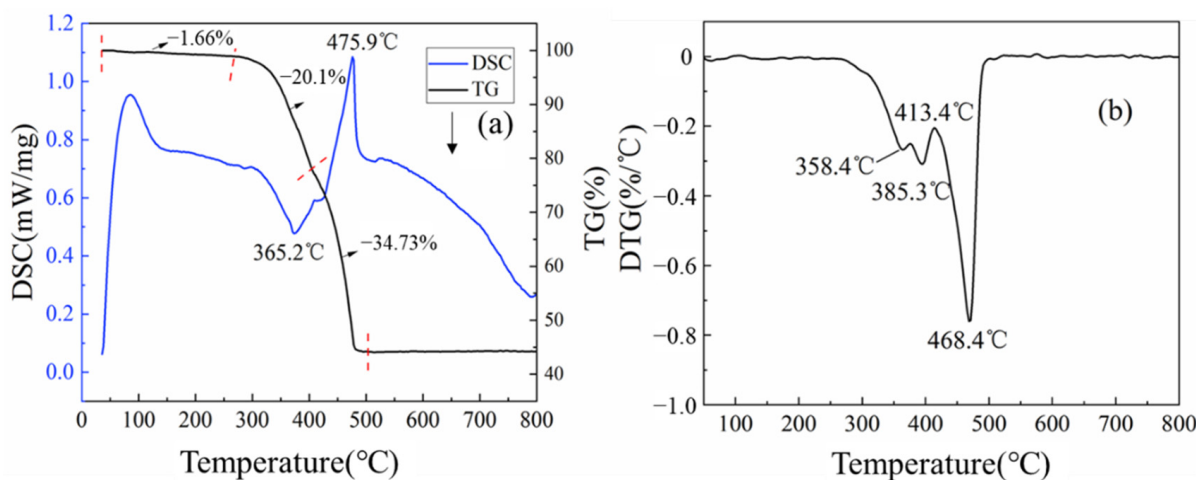


**Figure 5.** (a) TG -DSC curves of MAM; (b) DTG curves of MAM.

It can be seen from Figure 5a that DSC curves of MAM with two endothermic peaks and one exothermic peak at temperature range is from 30 °C to 500 °C. The first endothermic peak (<100 °C) can be attributed to the evaporation of free water and crystal water of MAM, which corresponded to a small amount of weightlessness. The exothermic peak (300–400 °C) can be attributed to the beginning of exothermic reaction (2), then the generated Hg (l) gasified at 357.3 °C, and SeO<sub>2</sub> (s) sublimated at 338.7 °C, with a little exothermic peak at the DSC curve. The endothermic peak between 400–500 °C can be attributed to the reaction (5) which absorbed a lot of heat, and HgSe was directly oxidized and decomposed into Hg (g) and SeO<sub>2</sub> (g). From the DTG curve in Figure 5b, the degree of gasification reached the maximum at 468.4 °C. With the rapid removal of Hg (g) and SeO<sub>2</sub> (g) by the protective gas, the reaction products were rapidly reduced, and this phenomenon intensified reaction (5) until all reactants HgSe disappear completely.

### 3.3. Heating Behavior and Dielectric Characteristics

As shown in Figure 6, microwave heating of MAM at 800 W was more effective than conventional heating at 2700 W. It only took 2.2 min for microwave heating of MAM to heat up from 20 °C to 500 °C, and the average heating rate was 227.27 °C /min, which was 3.79 times that of conventional heating. The rapid microwave heating of MAM can reduce the adsorption energy and the apparent activation energy, which was beneficial to the mercury removal process. Therefore, microwave intensified the pyrolysis of HgSe absorbed on the surface of MAM and made the mercury removal process more efficient and energy-saving.

The average heating rate of PbSO<sub>4</sub> (20 g) by microwave heating at 800 W was only 72.3 °C/min, which was far lower than that of MAM by microwave heating at 800 W (227.27 °C/min), so the rapid temperature rise of MAM in microwave field does not depend on PbSO<sub>4</sub>. The dielectric constant of MAM at room temperature was detected as 7.54, and the dielectric loss was 0.294. Both of the dielectric constant and dielectric loss of MAM were higher than that (dielectric constant: 4.6; dielectric loss:  $1.36 \times 10^{-4}$ ) of PbSO<sub>4</sub> which was the main phase after microwave heating treatment. Because MAM was mainly composed by HgSe and PbSO<sub>4</sub>, according to the mixture permittivity calculation equation as shown in Equation (6), the dielectric constant and dielectric loss of HgSe must be higher than that of MAM, which make the HgSe absorbed on the surface of PbSO<sub>4</sub> blocks is easier to be heated by microwave heating. For the microwave selective heating of HgSe (Figure 7), the absorption energy of HgSe on the surface of PbSO<sub>4</sub> blocks was reduced, and in this way the HgSe pyrolysis process was intensified.

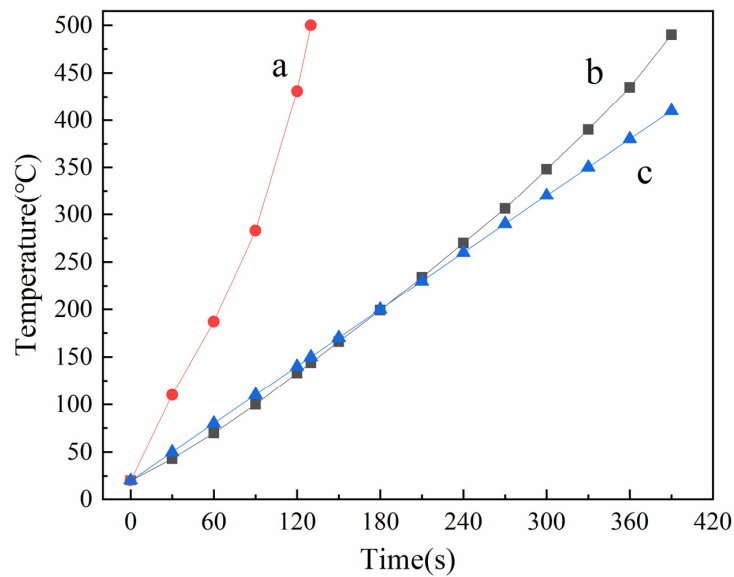


**Figure 6.** (a): Heating curve of MAM by microwave heating (800 W); (b): Heating curve of PbSO<sub>4</sub> (20 g) by microwave heating (800 W); (c): Heating curve of MAM by conventional heating (2700 W).

$$\epsilon' = \sum_{i=1}^n v_i \epsilon'_i + \sum_{i=1}^{n-1} \sum_{j=i+1}^n v_i v_j (\epsilon'_i - \epsilon'_j) \quad \text{for } \epsilon'_i > \epsilon'_j \quad (6)$$

where,  $\epsilon'$  = dielectric constant of the mixture;  $v_i$  = volume fraction of the  $i$ th constituent;  $\epsilon'_i$ ,  $\epsilon'_j$  = dielectric constant of the  $i$ th,  $j$ th constituent, respectively;  $n$  = number of constituents in the sample.

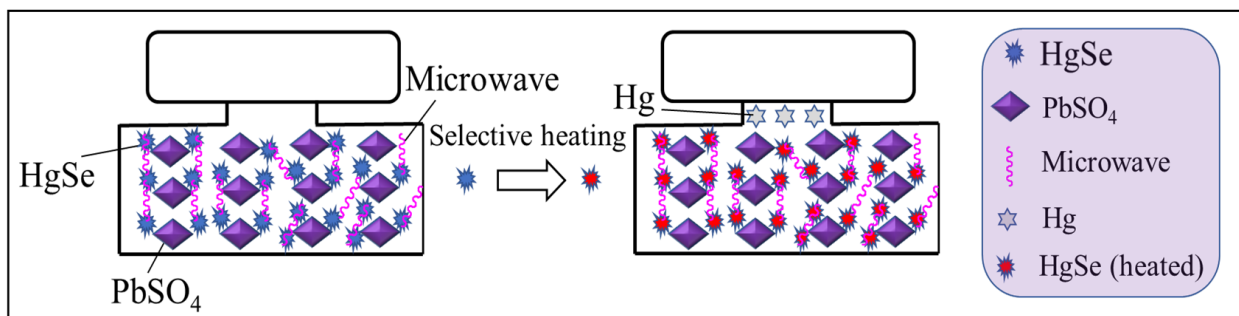


**Figure 7.** Mechanism diagram of the recovery of mercury from MAM by microwave heating.

### 3.4. The Recovery Rate of Mercury

According to the Equation (1), the calculation results of the mercury recovery rate are shown in Figure 8a. When the treating time was set to 30 min, the mercury recovery rate of both microwave heating and conventional heating increased with the increase in roasting temperature. When the microwave heating temperature was above 400 °C, the mercury recovery rate was more than 99.5%. While the mercury recovery rate of conventional heating was below 50% even when the roasting temperature was 500 °C. Therefore, the microwave heating was more effective for the recovery of mercury in MAM than conventional heating.

The reason for the high efficiency of mercury recovery from MAM by microwave heating was that HgSe adsorbed on the surface of PbSO<sub>4</sub> blocks was selectively heated by microwave, and the rapid desorption of HgSe was realized. The desorbed HgSe can pyrolyze rapidly, and the effective recovery of Hg<sup>0</sup> and Se (H<sub>2</sub>SeO<sub>3</sub> in water condenser). The strengthening mechanism of mercury recovery by microwave heating is shown in Figure 8b.

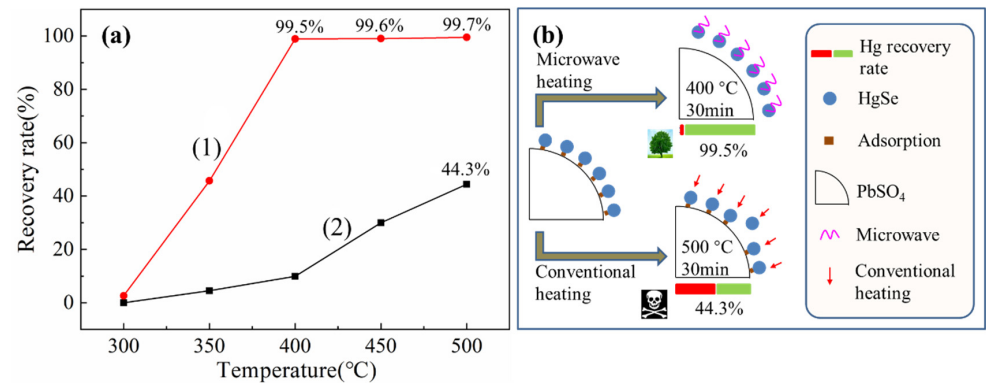


**Figure 8.** (a) Recovery rate of mercury by (a1) microwave heating, (a2) by conventional heating, and the (b) enhanced desorption mechanism diagram by microwave selective heating.

### 3.5. Characterization Results of Roasting Slag

Figure 9(a1) is the XRD results of MAM treated by microwave heating at 400 °C and conventional heating at 500 °C. By comparison, the mercury recovery effect of MAM by microwave heating was much better than that by conventional heating, because no HgSe phase was detected in MAM treated by microwave heating while there was still obvious HgSe phase by conventional heating as shown in (Figure 9(a2)).

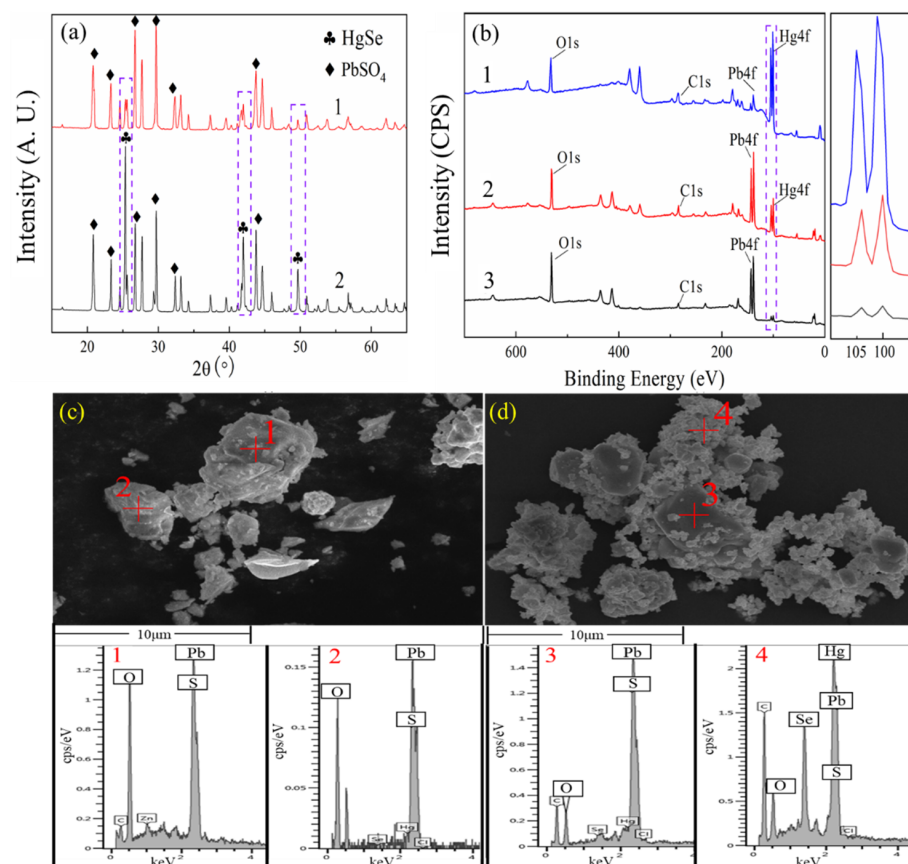


**Figure 9.** (a) XRD results of MAM by (a1) microwave heating at 400 °C and (a2) conventional heating at 500 °C; (b) The high-resolution XPS survey spectra of MAM: (b1) untreated MAM, (b2) MAM treated by conventional heating at 500 °C and (b3) MAM treated by microwave heating at 400 °C; (c) FESEM-EDS image of MAM treated by microwave heating at 400 °C; (d) FESEM-EDS image of MAM treated by conventional heating at 500 °C.

XPS detection results confirmed the conclusion that microwave heating had a better mercury recovery effect than that of conventional heating for intensity of Hg4f peaks decreased after conventional heating (Figure 9(b2)) while disappeared after microwave heating (Figure 9(b3)).

FESEM results also show that microwave heating had a better mercury recovery effect. As shown in FigX, the HgSe floc had been removed clearly from the surface of PbSO<sub>4</sub> blocks by microwave heating (Figure 9c) while there was still a lot of HgSe floc absorbed on the surface of PbSO<sub>4</sub> blocks by conventional heating (Figure 9d).

The advantage of mercury recovery of MAM by microwave heating can be summarized as follows: (1) Microwave heating can heat the HgSe selectively and achieve rapid heating to recovery mercury through HgSe pyrolysis. (2) Microwave can eliminate most of the adsorption energy of mercury compounds on the surface of the substrate, which can intensify the reactions through reducing the apparent activation energy of related reactions [27,35,36]. (3) Our previous research [37] also showed that the introduced gas was non-microwave absorbing and took away little heat in the microwave roasting process, and the energy of the microwave is mainly concentrated in the material, which means microwave heating was more energy saving than conventional heating.

### 3.6. Prototyping Technology

Based on the investigation results presented above, we proposed a proper process presented in Figure 10, to treat MAM by microwave heating, which can realize the recovery of Hg/Se/PbSO<sub>4</sub> efficiently and save energy. By adopting this process, HgSe in MAM was separated from the surface of PbSO<sub>4</sub> blocks; recovered as Hg<sup>0</sup> and H<sub>2</sub>SeO<sub>3</sub> in a water condenser; and the slag after microwave heating contained PbSO<sub>4</sub> above 92%, which can be recycled in lead smelting plants. Compared with different mercury recovery methods for MAM, the microwave heat treatment process has certain advantages (Table 2).

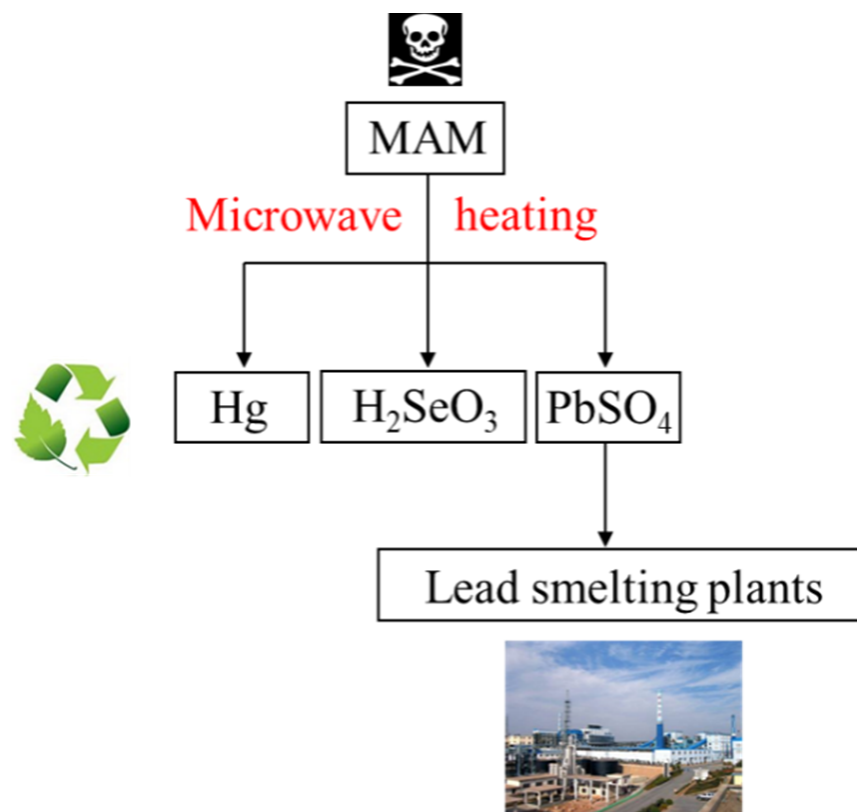


**Figure 10.** Hazard-free treatment of MAM and efficient recovery of metal by microwave.

**Table 2.** Effect of different treatment methods on mercury recovery of MAM.

Mercury Content of MAM (wt%)	Method	Temperature	Time	Hg Recover Rate	References
3%	Acid leaching	Room temperature	4 h	91.87%	[13]
10%	Acid leaching	80 °C	2 h	72.73%	[12]
1.37%	Thermal treatment	650 °C	1.5 h	99.4%	[11]
34.82%	Microwave heating	400 °C	0.5 h	99.5%	This work

#### 4. Conclusions

The main phases of MAM produced by zinc smelter are HgSe and PbSO<sub>4</sub>, and metal resources of MAM can be recovered by thermal treatment. In this paper, by comparing microwave heating with conventional heating, the enhancement effect of microwave field on the pyrolysis of HgSe adsorbed on the surface of PbSO<sub>4</sub> block was studied. The main conclusions are as follows:

(1) The pyrolysis of HgSe in MAM was conducted in air, and the main related reaction was:  $\text{HgSe} + \text{O}_2 = \text{Hg} + \text{SeO}_2$  (the pyrolysis process also included the phase change of Hg and SeO<sub>2</sub>). The thermogravimetry results show that the mercury removal temperature range of MAM was 300–500 °C.

(2) Heating behavior experiments and dielectric characteristics detection showed that the order of microwave heating effect is HgSe > MAM > PbSO<sub>4</sub>. Therefore, microwave could heat HgSe selectively, eliminate the most adsorption energy of HgSe on the surface of PbSO<sub>4</sub> block quickly, and strengthen the pyrolysis process of HgSe. When MAM was roasted at 400 °C for 30 min by microwave heating, the mercury recovery rate is more than 99.5%, which is far superior to conventional heating.

(3) Based on the microwave enhanced mercury removal process of MAM, the process flow of comprehensive recovery of Hg/Se/Pb from MAM was put forward, which was helpful to realize secondary resource recovery and the green production of lead-zinc smelting process.

**Author Contributions:** Conceptualization, H.Z. and K.Y.; methodology, H.Z. and L.Z.; software, P.L.; validation, H.Z., P.L. and Y.H.; formal analysis, H.Z. and P.L.; resources, L.Z.; writing—original draft preparation, H.Z.; writing—review and editing, H.Z. All authors have read and agreed to the published version of the manuscript.

**Funding:** This work was supported by Key Technology and Demonstration of Field-Oriented Decontamination and Reuse of Sour Acid/Sludge (grant number 2019YFC1904204), High-level Talent Discipline Construction Funding of Kunming University of Science and Technology (grant number 1411909512), and Yunnan Provincial Science and Technology Talents Program (grant number 202005AC160033).

**Institutional Review Board Statement:** Not applicable.

**Informed Consent Statement:** Not applicable.

**Data Availability Statement:** Not applicable.

**Conflicts of Interest:** The authors declare no conflict of interest.

#### References

1. Paula, A.; Marcello, M.V.; Bruce, G.M.; Tatiana, S.; Denise, C.R.E. Investigation of mercury cyanide adsorption from synthetic wastewater aqueous solution on granular activated carbon. *J. Water. Process. Eng.* **2020**, *34*, 101154.
2. Philip, O.; Ozuah, M.D. Mercury poisoning. *Curr. Prob. Pediatr.* **2000**, *30*, 91–99.
3. Zahir, F.; Rizwi, S.J.; Haq, S.K.; Khan, R.H. Low dose mercury toxicity and human health. *Environ. Toxicol. Phar.* **2005**, *20*, 351–360. [[CrossRef](#)] [[PubMed](#)]
4. Mukherjee, A.B.; Zevenhoven, R.; Brodersen, J. Mercury in waste in the European Union: Sources, disposal methods and risks. *Resour. Consvr. Recycl.* **2004**, *42*, 155–182. [[CrossRef](#)]

5. Ma, Y.P.; Du, J.J.; Zhang, X.M.; Li, Y.S. Research progress on mercury emission control technology from nonferrous metal smelting flue gas. *Guangzhou Chem. Ind.* **2016**, *44*, 13–17.
6. Hou, H.B. Analysis of mercury recovery process and production status in Shaoguan smelter. *Hunan. Nonferr. Metals.* **2001**, *17*, 15–20.
7. Loan, M.; Newman, O.M.G.; Cooper, R.M.G.; Farrow, J.J.; Parkinson, G.M. Defining the Paragoethite process for iron removal in zinc hydrometallurgy. *Hydrometallurgy* **2007**, *81*, 104–129. [[CrossRef](#)]
8. Ismael, M.R.C.; Carvalho, J.M.R. Iron recovery from sulphate leach liquors in zinc hydrometallurgy. *Miner. Eng.* **2003**, *16*, 31–39. [[CrossRef](#)]
9. Li, Z.L.; Xu, Z.F.; Zhang, X. Distribution of mercury resources and current situation of mercury removal in nonferrous metallurgy industry. *Nonferr. Metal Extr. Metall.* **2020**, *6*, 1–7.
10. Zhao, Q.Y.; Tong, L.; Zhou, X.S. Mercury pollution in China's Chloro-alkali industry and countermeasures. *Environ. Prot. Chem. Ind.* **2009**, *29*, 483–487.
11. Lei, X.; Zhong, Y.; Wu, H.G.; Niu, L. Separation and recovery of selenium and mercury from complex mercury bearing selenium residue. *Nonferr. Metal Extr. Metall.* **2017**, *4*, 48–51.
12. Zhou, S.; Zhong, Y.; Xiang, R.J. Study on extraction and separation technology of selenium and mercury from acid sludge. *J. Xiangtan. Univ.* **2020**, *42*, 86–94.
13. Zhang, W.L.; Wang, Y.Q.; Yu, Y.T.; Xu, Z.; Liu, X.J. Recovery of selenium and mercury from acid mud after wet dust collecting process in gold smelt. *Min. Metall. Eng.* **2017**, *5*, 96–99.
14. Ren, W.; Duan, L.; Zhu, Z.; Wen, D. Mercury transformation and distribution across a polyvinyl chloride (PVC) production line in China. *Environ. Sci. Technol.* **2014**, *48*, 2321–2327. [[CrossRef](#)]
15. Liu, J. Study on regeneration of waste mercury-containing catalysts by microwave activation. Ph.D. Thesis, Kunming University of Science and Technology, Kunming, China, 2019. [[CrossRef](#)]
16. Li, X.Y.; Pan, X.L.; Bao, X.H. Nitrogen doped carbon catalyzing acetylene conversion to vinyl chloride. *J. Energy Chem.* **2014**, *23*, 131–135. [[CrossRef](#)]
17. Liu, C.; Peng, J.H.; Liu, J.; Guo, P.; Wang, S.X.; Liu, C.H.; Zhang, L.B. Catalytic removal of mercury from waste carbonaceous catalyst by microwave heating. *J. Hazard. Mater.* **2018**, *358*, 198–206. [[CrossRef](#)]
18. Lam, S.S.; Chase, H.A. A Review on Waste to Energy Processes Using Microwave Pyrolysis. *Energies* **2012**, *57*, 1–24. [[CrossRef](#)]
19. Rodríguez-Jasso, R.M.; Mussatto, S.I.; Pastrana, L. Microwave-assisted extraction of sulfated polysaccharides (fucoidan) from brown seaweed. *Carbohydr. Polym.* **2012**, *86*, 1137–1144. [[CrossRef](#)]
20. Jones, D.A.; Lelyveld, T.P.; Mavrofidis, S.D.; Kingman, S.W.; Miles, N.J. Microwave heating applications in environmental engineering—A review. *Resour. Conserv. Recy.* **2002**, *34*, 75–90. [[CrossRef](#)]
21. Eliasson, L.; Isaksson, S.; Lövenklev, M.; Ahrné, L. A comparative study of infrared and microwave heating for microbial decontamination of paprika powder. *Front. Microbiol.* **2015**, *6*, 1071. [[CrossRef](#)]
22. Tyagi, V.K.; Lo, S.L. Microwave irradiation: A sustainable way for sludge treatment and resource recovery. *Renew. Sust. Energ. Rev.* **2013**, *18*, 288–305. [[CrossRef](#)]
23. Li, Y.; Chen, G.; Peng, J.; Srinivasakannan, C.; Ruan, R. Study of the oxygen reduction of low valent titanium in high titanium slag by microwave rapid heating. *Powder Technol.* **2017**, *315*, 318–321. [[CrossRef](#)]
24. Haque, K.E. Microwave energy for mineral treatment processes—A brief review. *Int. J. Miner. Process.* **1999**, *57*, 1–24. [[CrossRef](#)]
25. Luo, H.; Bao, L.; Kong, L.; Sun, Y. Low temperature microwave-assisted pyrolysis of wood sawdust for phenolic rich compounds: Kinetics and dielectric properties analysis. *Bioresour. Technol.* **2017**, *238*, 109–115. [[CrossRef](#)]
26. Huang, Y.F.; Chiueh, P.T.; Kuan, W.H. Microwave pyrolysis of lignocellulosic biomass: Heating performance and reaction kinetics. *Energy* **2016**, *100*, 137–144. [[CrossRef](#)]
27. Clark, D.E.; Folz, D.C.; West, J.K. Processing materials with microwave energy. *Mater. Sci. Eng. A* **2000**, *287*, 153–158. [[CrossRef](#)]
28. Rodríguez-Jasso, R.M.; Mussatto, S.I.; Pastrana, L.; Aguilar, C.N.; Teixeira, J.A. Chemical composition and antioxidant activity of sulphated polysaccharides extracted from *Fucus vesiculosus* using different hydrothermal processes. *Chem. Pap.* **2014**, *68*, 203–209. [[CrossRef](#)]
29. Busto, Y.; Cabrera, X.; Tack, F.M.G.; Verloo, M.G. Potential of thermal treatment for decontamination of mercury containing wastes from chlor-alkali industry. *J. Hazard. Mater.* **2011**, *186*, 114–118. [[CrossRef](#)]
30. Singh, N.; Patil, K.R.; Khanna, P.K. Nano-sized HgSe powder: Single-step preparation and characterization. *Mater. Sci. Eng. B.* **2007**, *142*, 31–36. [[CrossRef](#)]
31. Ding, T.; Zhang, J.R.; Hong, J.M.; Zhu, J.J.; Chen, H.Y. Sonochemical synthesis of taper shaped HgSe nanorods in polyol solvent. *Cryst. Growth. Des.* **2004**, *260*, 527–531. [[CrossRef](#)]
32. Zhang, Y.P.; Li, E.; Zhang, J.; Yun, C.Y.; Zheng, H.; Guo, G.F. A broadband variable-temperature test system for complex permittivity measurements of solid and powder materials. *Rev. Sci. Instrum.* **2018**, *89*, 024701. [[CrossRef](#)]
33. Liu, P.; Zhang, L.B.; Liu, B.G.; He, G.J.; Huang, M.Y. Determination of dielectric properties of titanium carbide fabricated by microwave synthesis with Ti-bearing blast furnace slag. *Int. J. Min. Met. Mater.* **2020**, *28*, 1–10. [[CrossRef](#)]

34. Amilton, B.B.J.; Denise, C.R.E.; Jorge, A.S.T. The use of computational thermodynamic for yttrium recovery from rare earth elements-bearing residue. *J. Rare. Earth* **2021**, *2*, 201–207.
35. Liu, P.; Liu, C.; Hu, T. Kinetic study of microwave enhanced mercury desorption for the regeneration of spent activated carbon supported mercuric chloride catalysts. *Chem. Eng. J.* **2020**, *408*, 127335. [[CrossRef](#)]
36. Liu, C.; Peng, J.; Ma, A.; Zhang, L.; Li, J. Study on non-isothermal kinetics of the thermal desorption of mercury from spent mercuric chloride catalyst. *J. Hazard. Mater.* **2017**, *322*, 325–333. [[CrossRef](#)]
37. Liu, P.; Liu, C.; Li, S.W.; Zhang, L.B.; Peng, J.H. Desorption kinetic study of mercury species in spent mercury chloride catalyst from polyvinyl chloride production process. *Environ. Prog. Sustain.* **2019**, *38*, 13201. [[CrossRef](#)]